Sinusoidal Perturbations Improve the Noise Behavior in Parallel EPI

M. Haeberlin[1], B. Wilm[1], C. Barmet[1], S. Kozerke[1], G. Katsikatsos[1], and K. P. Pruessmann[1]
[1]Department of Electrical Engineering, ETH Zurich, Zurich, Switzerland

Introduction

Parallel MRI permits decreased acquisition times by reducing the amount of k-space coverage needed for image reconstruction. However, when pushing the reduction factor, images suffer from spatially dependent noise amplification which potentially introduces features, that could be mistaken for structure and lead to image mis-interpretation. as (for Cartesian trajectories) described by the g-factor [1].

Generally, noise amplification depends on the interplay between k-space encoding strategy, B_1-sensitivities of the applied receive coil array and B_0. Since the invent of parallel imaging, multiple receive RF coil arrays have been optimized to achieve high reduction factors while keeping noise amplification tolerable. Furthermore, parallel imaging has gained from acquisition at increasingly higher field strengths.

Despite fast advances in parallel imaging hardware, k-space acquisition strategies have stayed limited to purely Cartesian reconstruction in clinical MRI. Non-Cartesian acquisition strategies hold the potential to achieve an improved noise behavior in the image. However, their sensitivity to B_0 offset, B_0 inhomogeneity as well as to other encoding imperfections prohibits obtaining image quality comparable to the images using Cartesian sampling schemes.

Recent improvements in NMR field monitoring [moni] have made it possible to monitor the field dynamics during spatial encoding.

By incorporating this information into image reconstruction, these artifacts can be removed.

In the present work we employ this newly available method to approach improved image noise properties by undersampled EPI trajectories whose phase encode lines are sine-shaped as opposed to purely Cartesian EPI. The effect of the sine-amplitude and randomness is assessed by simulations. In addition, experimental data in-vivo is presented.

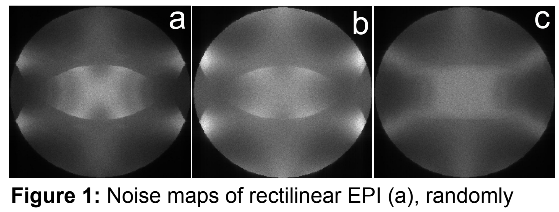

Figure 1: Noise maps of rectilinear EPI (a), randomly wiggled EPI (b), and sine-modulated EPI (c).

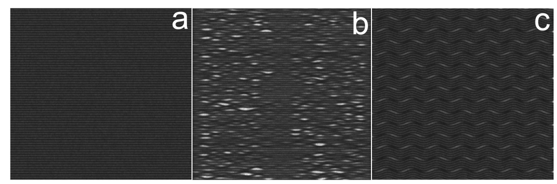

Theory and Methods: A desirable property of image noise is a homogeneous distribution across the image with a low maximum value. Image noise can be calculated by the image covariance matrix $\boldsymbol{X}$ given by $\boldsymbol{X} = \boldsymbol{F\psi F^H}$, where $\boldsymbol{F}$ denotes the reconstruction matrix, $\boldsymbol{\psi}$ reflects the receiver array's noise correlation matrix [ref SENSE] and $\boldsymbol{F^H}$ denotes the hermitian adjoint of $\boldsymbol{F}$. The off-diagonal elements of $\boldsymbol{X}$ reflect the noise cross-talk between pixels of the reconstructed image and its diagonal elements describe the noise variance of each pixel. The diagonal elements of $\boldsymbol{X}$ can be estimated by a series of images reconstructed from pure noise input signal for a given encoding setup. Simulations were carried out using Matlab™ 7.6 (MathWorks, Natick, MA*).* 80 instances of complex, white Gaussian noise were generated and fed into the iterative SENSE reconstruction **[3]**. Noise correlation $\boldsymbol{\psi}$ among the receiver channels was neglected. The final noise maps were calculated as the root-mean-square images over all 80 reconstructions.

Three trajectories were compared: Cartesian EPI, a randomly wiggled EPI and EPI with sine-modulated phase encoding lines. The amplitudes were chosen larger than reduction factor times $\Delta k_{Nyquist}$. All 3 trajectories were 3-fold undersampled and consisted of 5 interleaves. A circular 6-element array was used to mimic complex-valued coil sensitivitie*s.*

In-vivo measurement: Data were acquired on a Philips Achieva System (Philips, Best, The Netherlands) with a healthy volunteer. Protocol parameters were as follows: slice thickness = 2mm, FOV = $(264mm)^2$, in-plane resolution = $(1.1mm)^2$, flip angle = 30°.TR=1000ms, TE=21ms and T_{Acq}= 43ms per interleave. **Results:** The noise maps of the Cartesian EPI (Fig. 3a) show relatively strong maximum noise amplification (Fig. 1a) in the image domain and a largely varying spatial distribution, whereas noise in k-space is uniformly distributed (2a). The noise map (Fig. 1b) of the randomly wiggled trajectory (Fig. 3b) displays a larger maximum and slightly less structured noise (Fig. 1b) than the Cartesian EPI in the image domain. This is also visible in the k-space noise picture of the randomly wiggled EPI (Fig. 2b) which yield excessive noise amplification. The sine-modulated trajectory (Fig. 3c) exhibits a less structured spatial noise distribution (Fig. 1c) with reduced maximum noise value in the center as compared to the Cartesian EPI. In the corresponding k-space picture small gaps are also observed due to imperfect regularity of the implemented trajectory (Fig. 2c).

In-vivo measurement: Image reconstruction using the monitored trajectories were free from of aliasing artifacts as well as image ghosting (Fig. 4). Despite a 3-fold undersampling noise distribution does not show visual transitions within the image. The sine-modulated trajectory (Fig. 3c) was used to encode the in-vivo image and monitored (Fig. 5).

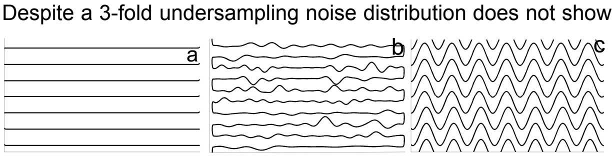

Figure 3: Trajectory associated with the noise maps in Figure 1

Discussion: It is shown that parallel imaging benefits from modulating EPI phase encoding lines. As opposed to Cartesian EPI (Fig. 3a), randomly wiggled phase encodes (Fig. 3b) can cause large gaps in k-space which cause inacceptable noise amplification. It is concluded that the modulations should occur in a highly coherent fashion, which is shown in simulations. Aliasing-free reconstruction of an undersampled multishot EPI trajectory with sine-modulations on the phase encoding lines are presented in-vivo.

The presented results promise great potential to significantly stabilize pMRI at high reduction factors. Field monitoring ensures that any well-suited trajectory can be used to further optimized the noise performance in the future.

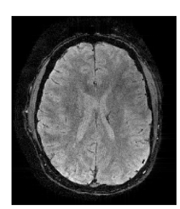

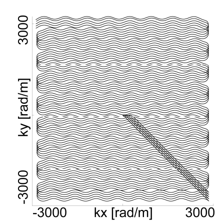

Figure 4 (left): Aliasing-free, monitoring-based SENSE reconstruction.
Figure 5 (right): Monitored k-space trajectory of the head scan.

References: **[1]** KP Pruessmann et al., MRM 42:952 (1999). **[2]** Barmet et al. MRM 60:187 (2008). **[3]** KP Pruessmann Et al., MRM 46:638 (2001).